

## **MATHEMATICAL MODELING**

### **3.0 General**

Uplift pressure distribution in cracks of the concrete gravity dam changes in time and space during changing reservoir level along either propagating or existing crack in concrete gravity dams. The effect of creep phenomenon in the FPZ is assumed to cause only temporal variation of crack mouth opening. The effect of creep in dam body or crack FPZ has been assumed to be negligible in present study of structural behavior of the concrete gravity dam. Creep phenomenon in a FPZ of given crack is influenced by interaction of multiple cracks, fatigue, alkali-silica-reaction (ASR), crack location and its geometry etc. The influence of these factors on FPZ-creep and hence CMOD rate are not available in literatures. Therefore, simplified CMOD rate function for single crack, taken from literatures, has been used as CMOD rate generating functions. This CMOD rate generating function is used in the solution of transient uplift pressure in cracks of the concrete gravity dam using 1-D mass and momentum equation, discussed in **Chapter 2**. The effect of this uplift on dam crown deflection has been accomplished through the FEM formulation of plane-strain linear elastic equations. Also factor of safety against sliding has been evaluated after considering these uplift pressures.

### **3.1 Transient Pressure in Single Crack**

Transient pressure variation in single cohesive crack is developed in present section. Transient nature of pressure is introduced through crack wall motion. The crack wall motion may be caused either by earthquakes, creep phenomenon in fracture process zone (FPZ) or fatigue due to reservoir level

variations. Crack length is assumed to be constant during each opening-closing cycle and it changes only from one cycle to another. Due to uncertain value of fracture toughness the crack length are assumed iteratively for each cycle.

### 3.1.1 Hydrodynamic Description of Water Flow with Moving Walls

Based on the test results for temporal and spatial pressure variation along the crack length of existing and new cracks, Javanmardi et. al. (2005a, 2005b) developed the hydraulics of one dimensional water flow in a single crack under moving impermeable walls (Javanmardi et. al. 2005a).

Due to pushing of the water by existing reservoir water pressure at crack mouth, water flows from crack mouth toward the crack tip during its first opening cycle in both existing and new cracks [Fig. 3.1(a)]. Water fills the voids developed due to crack opening and saturates completely the existing crack while propagating crack is saturated partially with saturation length  $L_{sp}$ . The magnitude of pressure varies along full length of existing crack but in propagating crack pressure decreases from reservoir pressure  $p_m$  at crack mouth to void pressure at the end of saturation length. The void is occupied by both water vapor and air. So the void pressure is determined by using certain thermodynamic equilibrium equations representing two-component single phase flow. But when there is no air in the concrete, the pressure decreases to water vapor pressure (cavitation) and water vapor fills the voids.

During crack closing, volume of the voids decreases due to squeezing out of water from existing crack [Fig.3.1 (a)] and propagating crack [Fig. 3.1(c)]. On increasing the crack closing velocity, the existing water is pressurized and now it flows in two opposite direction from a stagnation point along the

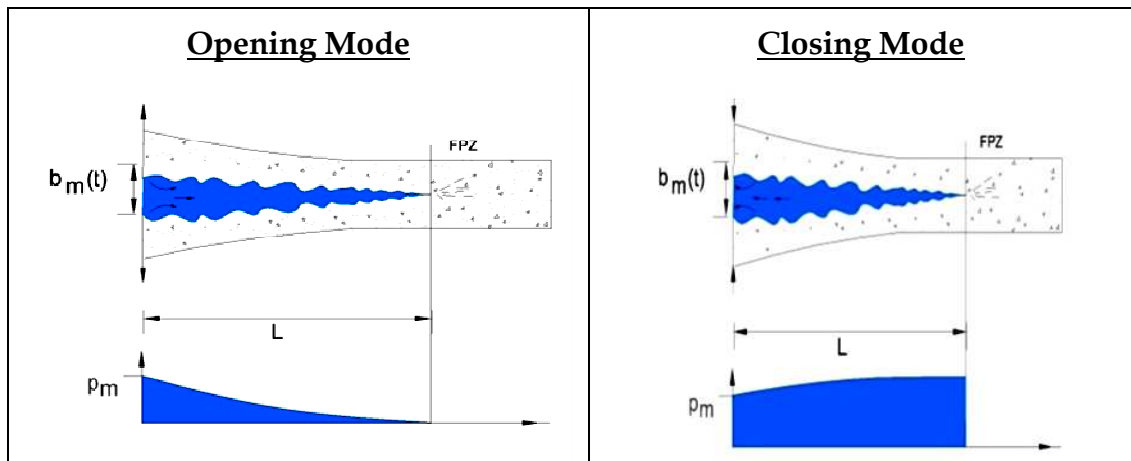


Fig.3.1(a). Water flow and pressure distribution in existing crack (Without Cavitation) with moving walls (Javanmardi et. al. 2005a).

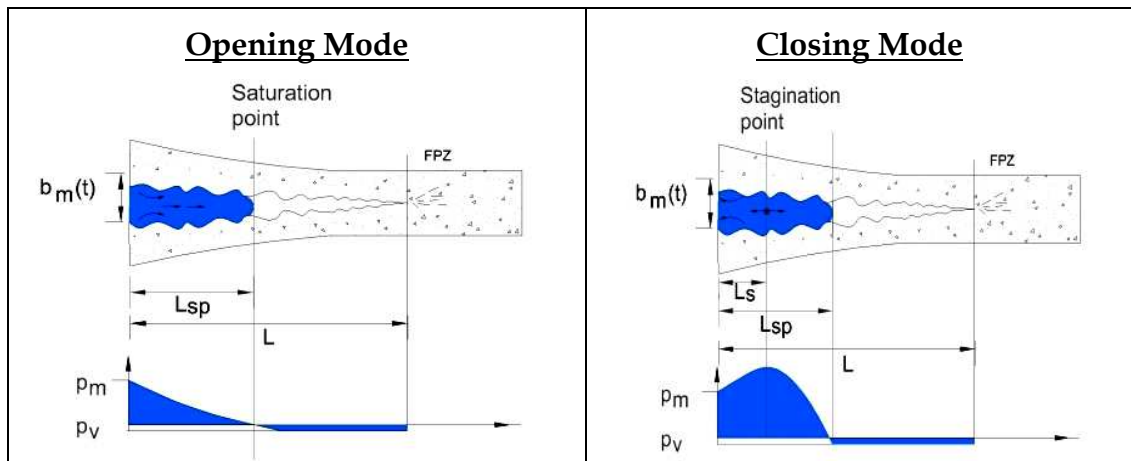


Fig.3.1(b). Water flow and pressure distribution in existing crack (With Cavitation) with moving walls (Javanmardi et. al. 2005a).

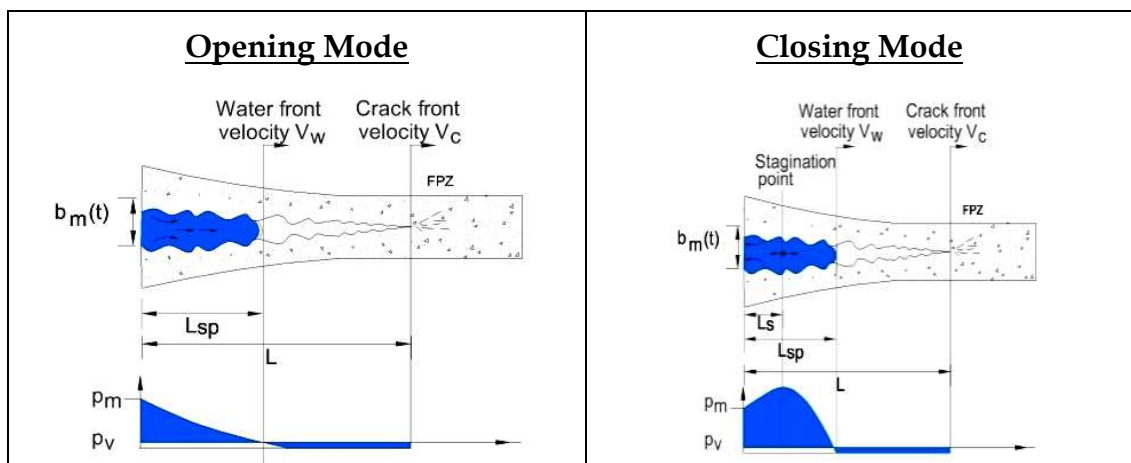


Fig.3.1(c). Water flow and pressure distribution in new crack with moving walls (Javanmardi et. al. 2005a).

saturation part of the crack in propagating crack while same phenomenon is found in existing crack after first opening -closing cycle [Fig.3.1 (b)]. The pressure at stagnation point is maximum and it decreases from this point toward the saturation region boundaries to become equal to the pressure at these two points.

In subsequent opening cycles, new voids are developing along propagating crack with water flow along crack from mouth toward crack tip during opening cycle. Water flow can only fill the voids close to the crack mouth and saturation length decreases. The only difference between the first opening and subsequent opening cycles is the existence of some water in residual opening that was already filled due to crack closing.

The water flow and corresponding pressure during second and subsequent cycle is therefore similar to that of the first closing cycle except that there is already some water in wetted unsaturated region. Thus saturation length may be longer at the end of the second closing cycle.

The case of propagating crack with saturated and unsaturated part is basically similar to an existing crack when cavitation occurs.

### **3.1.2 Mathematical Modeling of Transient Uplift Pressure in Cracks with Moving Walls**

Javanmardi et. al. (2005b) developed a theoretical modeling using the momentum equations proposed by Louis (1968) and discussed in Wittke (1990) for un- penetrated wedge shaped existing cracks under the following assumptions (Fig. 3.2).

- Walls of the crack are impermeable and rigid. This assumption can be introduced as the fluid permeability of cracks is significantly higher than that of un-cracked concrete.
- Flow is one dimensional along straight length of wedge crack.

- Water compressibility is negligible.
- The flow in unsaturated part is insignificant.
- Water vapor pressure is zero.
- Density of water  $\rho$  is independent of space.
- There is no sink or source.
- Lower wall of the crack is fixed and only upper wall moves.
- Crack wall stiffness is constant.
- Crack width is of unit dimension.
- Crack length is fixed.
- Velocity head gradient is neglected in both laminar and turbulent flow.
- Flow in crack is a single phase flow and there is no interaction between air and water.

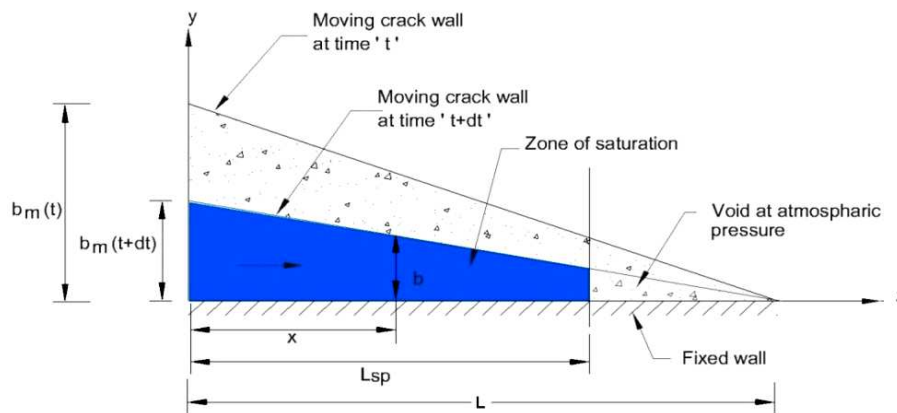


**Fig.3.2. Assumed crack in opening mode.**

The theoretical modeling of Javanmardi et. al. (2005b) lacks sufficient number of boundary conditions and solution scheme to calculate the unknown flow parameters by trial and error procedures has been suggested.

In present study, mathematical modeling of uplift pressure is carried out and supplemented with sufficient number of boundary conditions and Reynolds transport equation for mass conservation during closing phase of the crack,

to solve unknown parameters (e.g. stagnation pressure etc.) which are necessary to calculate complete pressure field in cracks at any time.

### 3.1.2.1 Continuity Equation

#### *Opening Mode*

1-D continuity equation, widely used by various workers (e.g. Slowik and Saouma, 2000; Sarris and Papanastasiou, 2012 etc.), is written with assumption that fluid leakage through walls of the crack are negligible (i.e. walls of the crack are impermeable). For any cross sectional area  $A$  of the crack, normal to flow direction  $x$ , the 1-D continuity equation can be written as

$$\frac{\partial(\rho Q)}{\partial x} = \frac{\partial(\rho A)}{\partial t} \quad (3.1)$$

Where,  $Q$  is the discharge through the crack.

Considering unit thickness, equation (3.1) can be modified as:

$$\rho \frac{\partial Q}{\partial x} + \frac{\partial(\rho b)}{\partial t} = 0 \quad (3.2)$$

Where  $b$  is the crack opening at any distance  $x$  from the crack mouth and time  $t$ . Neglecting the water compressibility, equation is further simplified as

$$\frac{\partial Q}{\partial x} + \frac{\partial b}{\partial t} = 0 \quad (3.3)$$

For rigid crack wall

$$b = b_m \left(1 - \frac{x}{L}\right) \quad (3.4)$$

Where  $b_m$  crack mouth opening displacement (CMOD) and  $L$  is the crack length.

Using value of  $b$  in equation (3.4) and boundary condition, that at  $x = L_{sp}$  (saturation length),  $Q = 0$ ; equation (3.3) can be integrated as

$$Q = \frac{\dot{b}_m}{L} \left[ L(L_{sp} - x) - \frac{1}{2}(L_{sp}^2 - x^2) \right] \tag{3.5}$$

Where  $\dot{b}_m$  is the crack mouth opening displacement rate (CMOD rate). The equation gives discharge equation for flow in wedge shaped rigid crack in a concrete gravity dam during crack opening mode.

**Closing Mode**

During the closing phase, there occurs a point along the crack where discharge becomes zero. This point is called stagnation point. Water moves in both the direction from the stagnation point during the closing process of crack mouth. The distance of the point from the crack mouth is termed as stagnation length and denoted as  $L_s$  as shown in Fig.3.3.

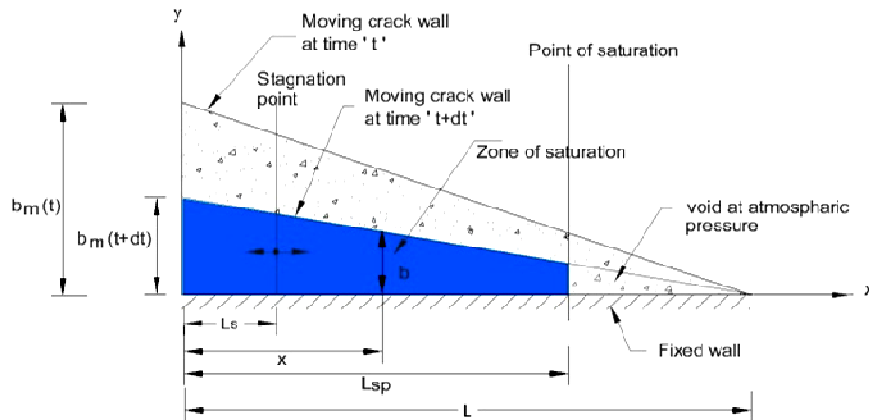


**Fig.3.3. Assumed crack in closing mode**

The discharge formula given by equation is modified for closing mode after using the boundary condition that at  $x = L_s, Q = 0$ .

$$Q = \frac{\dot{b}_m}{L} \left[ L(L_s - x) - \frac{1}{2}(L_s^2 - x^2) \right] \quad (3.6)$$

The equation (3.6) gives discharge equation for flow in wedge shaped rigid crack in a concrete gravity dam during crack closing mode.

### 3.1.2.2 Momentum Equation

Work of Louis (1969) as discussed in **Chapter-2**, has been utilized for present formulation. Javamardi et. al. (2005a) have shown that the relative roughness  $\frac{\varepsilon}{D_h} = 0.5$  is a good approximation for concrete cracks. Therefore, for this relative roughness value, the crack is assumed to be hydraulically rough ( $\frac{\varepsilon}{D_h} > 0.033$ ). Louis (1969) flow diagram shows that hydraulic zone IV (laminar flow) and hydraulic zone V (turbulent flow) are applicable for hydraulically rough crack. Flow changes from laminar to turbulent at Reynolds number ( $R_e = 2Q/\nu$ ) nearly 2300. The momentum equations are written for laminar and turbulent flow separately according Louis (1969; Table 2.1).

#### *Laminar Flow*

$$n = 1$$

$$K = \frac{gb^2}{12\nu \left[ 1 + 8.8 \left( \varepsilon / D_h \right)^{1.5} \right]} \quad (3.7)$$

Where,  $\nu$  kinematic viscosity of water and  $K$  is the hydraulic conductivity. Therefore, for laminar flow Louis (1969) momentum equation becomes

$$Q = -KbJ \quad (3.8)$$

Where,  $J = \frac{\partial H_T}{\partial x}$  is hydraulic gradient and  $H_T$  is the total head given by



$$H_T = z + \frac{p}{\gamma} + \frac{v^2}{2g} \quad (3.9)$$

Here  $z$  is location of crack which is fixed. On assumption that velocity head is negligible,

$$J = \frac{\partial H_p}{\partial x} = \frac{1}{\gamma} \frac{\partial p}{\partial x} \left( \frac{\partial z}{\partial x} = 0 \right) \quad (3.10)$$

Where,  $H_p$  is now pressure head, therefore, equation simplifies to

$$Q = -C_2 b^3 \frac{\partial p}{\partial x} \quad (3.11)$$

Where

$$C_2 = \frac{g}{12\nu\gamma \left[ 1 + 8.8(\varepsilon/D_h)^{1.5} \right]} \quad (3.12)$$

### ***Turbulent Flow***

$$\left. \begin{aligned} n &= 0.5 \\ K &= 4\sqrt{g} \log \left[ \frac{1.9}{\varepsilon/D_h} \right] \sqrt{b} \end{aligned} \right\} \quad (3.13)$$

Therefore, for turbulent flow Louis (1969) momentum equation becomes

$$Q = -KbJ^{0.5} \quad (3.14)$$

After inserting the values of  $K$  and  $J$  in equation (3.14), the resulting equation is

$$Q^2 = C_3 b^3 \frac{\partial p}{\partial x} \quad (3.15)$$

Where,

$$C_3 = \left( \frac{16g}{\gamma} \right) \log \left[ \frac{1.9}{(\varepsilon/D_h)} \right]^2 \quad (3.16)$$

### 3.3 Transient Pressure Calculation and Boundary Conditions

For the sake of clarity  $\left(\frac{dp}{dx}\right)_l$  and  $\left(\frac{dp}{dx}\right)_t$  are used respectively, for laminar and turbulent pressure gradients in subsequent discussions. Pressure calculation starts from the determination of opening ( $\dot{b}_m \geq 0$ ) and closing ( $\dot{b}_m < 0$ ) mode of the crack. The respective continuity and momentum equations for laminar and turbulent flows are coupled together when solving the differential equation for pressure. The laminar and turbulent flow regions are separated by transition lengths. It is assumed that when Reynolds number  $R_e \leq 2300$  then flow is laminar otherwise flow is turbulent. These criteria can be used to find the transition lengths or it can be calculated iteratively. Pressure in crack varies from hydrostatic pressure at mouth to vapor pressure (taken as zero) at the tip of crack. Considering these factors in mind the integral equations of pressure are written separately for opening and closing mode.

#### 3.3.1 Opening Mode

In the opening mode, laminar flow occurs near the crack mouth. The position where laminar flow changes to turbulent flow are denoted by  $L_t$ .  $L_t$  is calculated using expressions for Reynolds number and continuity equation (3.5) for opening mode. The integral equations for variation of pressure along the crack is written as

$$P(x,t) = \begin{cases} p_m + \int_0^x \left(\frac{dp}{dx}\right)_l dx & (0 \leq x \leq L_t) \\ p_m + \int_0^{L_t} \left(\frac{dp}{dx}\right)_l dx + \int_{L_t}^x \left(\frac{dp}{dx}\right)_t dx & (L_t \leq x \leq L_{sp}) \end{cases} \quad (3.17)$$

Here  $L_{sp}$  is the saturation length of crack where the pressure at any given time is assumed to be zero. Using this condition the  $L_{sp}$  is calculated as

$$p_m + \int_0^{L_t} \left( \frac{dp}{dx} \right)_l dx + \int_{L_t}^{L_{sp}} \left( \frac{dp}{dx} \right)_t dx = 0 \quad (3.18)$$

### 3.3.2 Closing Mode

In closing mode, flow starts from stagnation point in both upstream and downstream directions. Flow is laminar near the stagnation point. With the help of Reynolds expression and continuity equation (3.6) for closing mode, two transition lengths  $L_{tu}$  and  $L_{td}$  can be calculated where change of flow from laminar to turbulent occurs. Denoting the stagnation length and stagnation pressure by  $L_s$  and  $p_s$  respectively, the pressure variation for upstream ( $x \leq L_s$ ) and downstream ( $x > L_s$ ) can be written as follows.

*Pressure in upstream section ( $x \leq L_s$ )*

$$P(x, t) = \begin{cases} p_m + \int_0^x \left( \frac{dp}{dx} \right)_t dx & (0 \leq x \leq L_{tu}) \\ p_m + \int_0^{L_{tu}} \left( \frac{dp}{dx} \right)_t dx + \int_{L_{tu}}^x \left( \frac{dp}{dx} \right)_l dx & (L_{tu} \leq x \leq L_s) \end{cases} \quad (3.19)$$

*Pressure in downstream section ( $x > L_s$ )*

$$P(x, t) = \begin{cases} p_m + \int_0^{L_{tu}} \left( \frac{dp}{dx} \right)_t dx + \int_{L_{tu}}^{L_s} \left( \frac{dp}{dx} \right)_l dx + \int_{L_s}^x \left( \frac{dp}{dx} \right)_t dx & (L_s \leq x \leq L_{td}) \\ p_m + \int_0^{L_{tu}} \left( \frac{dp}{dx} \right)_t dx + \int_{L_{tu}}^{L_s} \left( \frac{dp}{dx} \right)_l dx + \int_{L_s}^{L_{td}} \left( \frac{dp}{dx} \right)_l dx + \int_{L_{td}}^x \left( \frac{dp}{dx} \right)_t dx & (L_{td} \leq x \leq L_{sp}) \end{cases} \quad (3.20)$$

In the above set of equations,  $L_s$ ,  $p_s$  and  $L_{sp}$  are unknown parameters and can be determined by using two boundary conditions and Reynolds transport theorem for mass conservation as follows:

*First boundary condition*

When  $x = L_s$  then  $p = p_s$  and therefore

$$p_m + \int_0^{L_{tu}} \left( \frac{dp}{dx} \right)_t dx + \int_{L_{tu}}^{L_s} \left( \frac{dp}{dx} \right)_l dx = p_s \quad (3.21)$$

**Second boundary condition**

When  $x = L_{sp}$  then  $p = 0$  and hence

$$p_m + \int_0^{L_{tu}} \left( \frac{dp}{dx} \right)_t dx + \int_{L_{tu}}^{L_s} \left( \frac{dp}{dx} \right)_l dx + \int_{L_s}^{L_{td}} \left( \frac{dp}{dx} \right)_l dx + \int_{L_{td}}^{L_{sp}} \left( \frac{dp}{dx} \right)_t dx = 0 \quad (3.22)$$

**Reynolds transport equation for mass conservation**

As per Reynolds transport equation, given by White (1994), the mass conservation law for the elemental control volume can be written as

$$\left( \frac{dm}{dt} \right) = \frac{d}{dt} \iiint \rho dV + \iint \rho(\mathbf{v} \cdot \mathbf{n}) dA = 0 \quad (3.23)$$

Where  $m$  and  $\rho$  are mass and density of water respectively;  $\mathbf{v}$  is the water velocity vector and  $\mathbf{n}$  is the outward unit normal vector on elemental surface  $dA$  of elemental control volume  $dV$ .

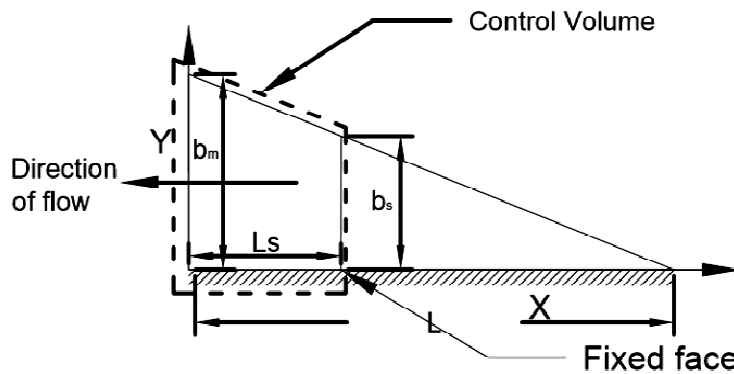


**Fig.3.4. Control volume for calculation of stagnation point**

For the present case a control volume lying between crack mouth and stagnation point (Fig.3.4) is assumed. Applying the above equation and noting that at stagnation point velocity of water is zero, the equation (3.23) yields

$$\frac{d}{dt} \left\{ \frac{1}{2} L_s b_m \left( 2 - \frac{L_s}{L} \right) \right\} + Q_m = 0 \quad (3.24)$$

Where  $Q_m$  is the discharge at crack mouth given by

$$Q_m = -\frac{\dot{b}_m}{2L} (2LL_s - L_s^2) \quad (3.25)$$

The equation (3.23) is first differentiated w.r.t. time and then solved by method of separation of variables with the condition that  $L_s = L$  when  $b_m = b_{mr}$ . The resulting expression is

$$L_s = L - L \sqrt{\left( 1 - \frac{b_{mr}}{b_m} \right)} \quad (3.26)$$

Equations (3.21), (3.22) and (3.26) are solved together for  $L_s$ ,  $p_s$  and  $L_{sp}$ . With these now known values, the set of equations (3.19) and (3.20) are solved to get the pressure distribution along the crack.

### 3.4 Calculation of Uplift Force in Cracks

Uplift force in the crack is calculated by integrating  $P(x, t)$  for both opening and closing modes.

$$F(t) = \int_0^L P(x, t) dx \quad (3.35)$$

Where,  $F(t)$  is uplift force in the crack at any time  $t$ .

### 3.5 Dam-crown Deflection Formulation

Generally it is believed that no-tension plastic design of the dam is on safer side. However, results of finite element analysis of complex dam geometries (Gioia et. al. 1992) showed that differences between plasticity and fracture

mechanics are more pronounced for the case when water penetrates into the crack and applies pressure on the concrete. However, in these studies, the effect of transient pressure variation along the crack on dam-crown deflection has not been reported. In the present study, effect of transient pressure variation on horizontal dam-crown deflection is formulated under certain set of assumptions.

### 3.5.1 Assumptions

- Crack length remains constant during each opening-closing cycle.
- Linear elastic fracture mechanics (LEFM) is applicable with plane strain condition.
- Concrete is homogeneous and isotropic.

### 3.5.2 Plane Strain Elastic Equation

Since axis length of the dam is very large in comparison to sectional dimensions of the dam, therefore, plane strain formulation with unit thickness is applicable for present case. For the case of plane strain, all the strain related to z-axis (along the dam length) vanish.

$$\epsilon_{zz} = \epsilon_{yz} = \epsilon_{zx} = 0 \quad (3.36)$$

Here strain  $\epsilon$  is defined in terms of displacement vector  $\mathbf{u}$  as follows (Tauchert 1974).

$$\epsilon_{jk} = \frac{1}{2} \left( \frac{\partial u_j}{\partial x_k} + \frac{\partial u_k}{\partial x_j} \right) \quad (3.37)$$

Where,  $j, k = 1, 2, 3$  represent the component along the orthogonal  $x, y, z$  axis respectively. Linear stress-strain constitutive relation in tensor form can be written as

$$\sigma_{ij} = 2\mu\epsilon_{ij} + \lambda\delta_{ij}\epsilon_{kk} \quad (3.38)$$

Where,  $\sigma_{ij}$  are stresses in the direction of  $j$  on plane normal to  $i$ ;  $\delta_{ij}$  is Kronecker delta defined as

$$\delta_{ij} = \begin{cases} 1 & \text{if } i = j \\ 0 & \text{if } i \neq j \end{cases} \quad (3.39)$$

And,  $\mu$  and  $\lambda$  are Lamé constants which, for Elastic Modulus  $E$  and Poisson ratio  $\nu_0$ , are given as

$$\begin{aligned} \mu &= \frac{E}{2(1+\nu_0)} \\ \lambda &= \frac{E\nu_0}{(1+\nu_0)(1-2\nu_0)} \end{aligned} \quad (3.40)$$

Equation (3.38) is inverted and simplified using the equation (3.40), which gives

$$\epsilon_{ij} = \frac{1}{E} \{ (1+\nu_0)\sigma_{ij} - \nu_0\delta_{ij}\sigma_{kk} \} \quad (3.41)$$

Applying the conditions of plane strain (Equ. (3.36)) in equation (3.41) stress-strain relation in matrix notation can be written as

$$\begin{Bmatrix} \epsilon_{xx} \\ \epsilon_{yy} \\ \epsilon_{xy} \end{Bmatrix} = \frac{(1+\nu_0)}{E} \begin{bmatrix} (1-\nu_0) & -\nu_0 & 0 \\ -\nu_0 & (1-\nu_0) & 0 \\ 0 & 0 & 1 \end{bmatrix} \begin{Bmatrix} \sigma_{xx} \\ \sigma_{yy} \\ \sigma_{xy} \end{Bmatrix} \quad (3.42)$$

Equation (3.42) can be written in abbreviated form as

$$\{\epsilon\} = [D]\{\sigma\} \quad (3.43)$$

Or by inversion equation (3.43) can be transformed to

$$\{\sigma\} = [C]\{\epsilon\} \quad (3.44)$$

Where  $[C] = [D]^{-1}$ .

### 3.5.3 Plane Strain Energy Equation

The strain energy in three- dimensional space may be written as

$$U = \iiint \{\epsilon\}^T \{\sigma\} dV \quad (3.45)$$

Equation (3.45) can be written in unabridged notation for Plane strain condition as

$$U = \iiint \left[ \frac{E\nu_0}{2(1+\nu_0)(1-2\nu_0)} (\epsilon_{xx} + \epsilon_{yy})^2 + \frac{E}{2(1+\nu_0)} (\epsilon_{xx}^2 + \epsilon_{yy}^2 + 2\epsilon_{xy}^2) \right] dV \quad (3.46)$$

### 3.5.4 Triangular Plane Strain Finite Element

For problem domain having curved or straight edges with other than 90° angles, elements of triangular shape are preferable (Yang, 1990). Dam section belongs to this kind of problem domain. In this section a six degree of freedom, triangular plane strain finite element is formulated based on the following assumptions.

- Within each element, lines initially straight remain straight in their displaced position.
- The plane strains are assumed to be constant within each element.
- The element stresses are replaced by stress resultants which act at the corners of the element.

A three noded triangular element with two degree of freedom at each node has been taken for deriving the stiffness equation. In displaced position horizontal and vertical displacement of a node  $j$  is represented by  $(u_j, v_j)$ . Based on the linear displacement assumption, the displacement at any point  $(x, y)$  can be described by the following linear functions.



$$\left. \begin{aligned} u(x, y) &= u_0 + a_1x + a_2y \\ v(x, y) &= v_0 + a_3x + a_4y \end{aligned} \right\} \quad (3.47)$$

Where,  $u_0, v_0, a_1, a_2, a_3, a_4$  are displacement constants. These six displacement constants can be obtained in terms of nodal point displacement and geometry of the element by using nodal point displacement conditions. Using equations (3.37) and (3.47), strain displacement relation can be written as

$$\{\epsilon\}^T = \{q\}^T [A]^T \quad (3.48)$$

Where,  $\{\epsilon\}$  is strain vector;  $\{q\}$  is nodal displacement vector and  $[A]$  is the coefficient matrix.

### 3.5.5 Derivation of Element Stiffness Matrix

The element stiffness matrix can be derived after performing the partial differentiation of the strain energy with respect to each degree of freedom, following Castigliano's theorem. The strain energy for unit thickness triangular element can be written in the following form.

$$U = \iint \{\epsilon\}^T \{\sigma\} dA \quad (3.49)$$

Where,  $U$  is strain energy and  $\{\sigma\}$  is stress vector.

Using equation (3.44) and (3.48), the stress-displacement relation can be written as

$$\{\sigma\} = [C][A]\{q\} \quad (3.50)$$

Substituting equations (3.48) and (3.50) into equation (3.49), we have

$$U = \{q\}^T \left[ \iint [A]^T [C][A] dA \right] \{q\} \quad (3.51)$$

Applying the Castigliano's first theorem

$$F_i = \frac{\partial U}{\partial q_i} \tag{3.52}$$

Where,  $F_i$  is the force in direction of  $i$ . By performing partial differentiation of the strain energy with respect to each of the six degree of freedom of the finite element, we finally obtain

$$\{F\} = [k]\{q\} \tag{3.53}$$

Where,  $\{F\}$  is force vector and  $[k]$  is stiffness matrix defined as

$$[k] = \iint [A]^T [C][A] dA \tag{3.54}$$

### 3.5.6 Boundary Conditions for Dam- Crown Deflection

Boundary conditions are written separately for (a) uplift pressures at dam foundation, (b) uplift pressure in cracks in the dam body, (c) hydrostatic pressure at upstream face of the dam and (d) dam foundation displacement (Fig.3.5).

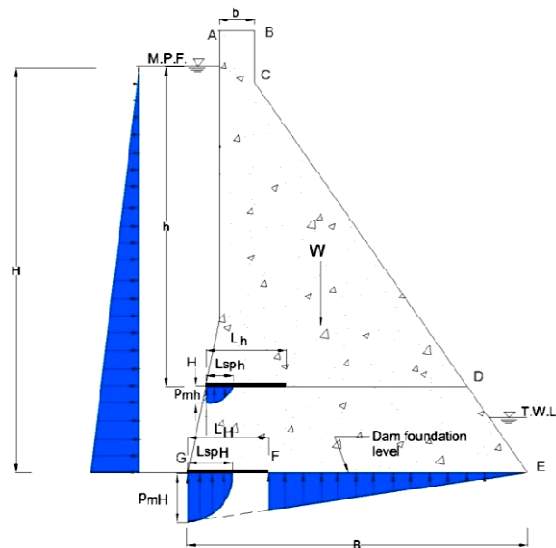


Fig.3.5. Boundary conditions for dam-crown deflections.

**(a) Dam Foundation uplift pressure**

At dam foundation interface, uplift force in crack portion as calculated by present model is applied. In un-cracked portion of the section along the crack, triangular uplift force due to seepage is assumed.

$$F(t) = \begin{cases} \int_0^{L_{spH}} p(x,t) dx \\ \frac{P_{mH}}{B} \int_L^B (B-x) dx \\ 0 \quad \text{elsewhere} \end{cases} \quad (3.55)$$

**(b) Uplift force in dam-body crack**

Uplift force on the section taken along the crack located in the dam body is divided into two part (a) crack portion and (b) un-cracked portion. Uplift force in the crack portion is calculated using the result of uplift pressure of present model. In un-cracked portion, zero uplift force is assumed. For section length  $B'$ , the uplift pressure can be written as:

$$F(t) = \begin{cases} \int_0^{L_{sph}} p(x,t) dx \\ 0 \quad \text{elsewhere} \end{cases} \quad (3.56)$$

**(c) Hydrostatic force at upstream face of the dam**

Triangular hydrostatic pressure variation is assumed at the upstream face of the dam. Therefore, horizontal force acting on the upstream force can be written as

$$F_H(t) = \int_0^H \gamma x dx \quad (3.57)$$

**(d) Dam foundation displacement**

Foundation of the dam is assumed to be rigid.

$$(u, v) = (0, 0) \quad \text{when} \quad y = 0 \quad (3.58)$$

**3.6 Factor of Safety against Sliding**

The sliding stability is based on a factor of safety as a measure of determining the resistance of the structure against sliding. In present study sliding factor of safety as recommended by USACE (1995) has been used. Assuming zero cohesion, sliding factor of safety can be written as

$$F_s = \frac{\mu_0 \sum V_0(t)}{\sum H_0} \quad (3.59)$$

Where,  $F_s$  is sliding factor of safety,  $\mu_0$  is friction coefficient,  $\sum V_0(t)$  is the summation of vertical forces acting on the dam (including uplift forces) and  $\sum H_0$  is the summation of horizontal forces acting on the dam. The factor of safety is calculated for following two cases of transient uplift pressure in the cracks.

- USACE (1995) criteria of no-change in uplift pressure during reservoir level variation. Uplift pressure at section varies from full reservoir level at upstream face to zero at downstream face of the dam.
- Uplift pressure variations in cracks as calculated in present study during reservoir level variation are considered. However at intact portion of the section passing through crack, the uplift pressure is assumed to be zero.

Sliding factor of safety, calculated for abovementioned two cases are computed and compared. In either of two cases, in addition to uplift forces in cracks, following set of forces are considered:

1. Dam body force.
2. Linear hydrostatic pressure variation at upstream face of the dam.
3. Tail water pressure is assumed to zero.
4. Silt pressure is zero.
5. Drains are in-operative.

### 3.7 Summary

One dimensional mathematical modeling of transient uplift pressure in the single wedge-shaped crack has been done on the basis of various assumptions and understanding of hydrodynamic phenomenon occurring during crack-wall motion. One dimensional continuity and Louis (1969) momentum equations for different flow regimes (laminar/ turbulent) and hydraulic roughness have been coupled separately for opening and closing phases of crack-wall motion. The resulting partial differential equations contains unknown pressure as function of space and time together with some important unknown parameters like saturation length, stagnation point and stagnation pressure. These unknown parameters are first solved using known or assumed boundary conditions and equation resulting from application of Reynolds transport equation of mass conservation to control volume chosen between crack mouth and stagnation point during closing phase. After calculating these flow parameters, partial differential equations are written in integral form separately for opening and closing mode to calculate pressure field at any given time.

For the dam, plane strain linear elastic equations have been developed, after assuming that LEFM is applicable for cracks in concrete gravity dams. A six degree of freedom triangular plane strain finite element is formulated. The element stiffness matrix is derived after performing the partial differentiation of the strain energy with respect to each degree of freedom following Castigliano's theorem. Boundary conditions are written separately for (a)

transient uplift pressures at dam foundation, (b) transient uplift pressures in cracks in the dam body and (c) hydrostatic pressure at upstream face of the dam.

In present study, sliding factor of safety as recommended by USACE (1995) is has been used assuming that concrete cohesion is zero. Sliding factor of safety is calculated separately for two uplift pressure conditions in cracks: (i) Uplift pressure distribution as recommended by USACE and (ii) Uplift pressures in present study.